Journal of Computational Physics 228 (2009) 8301–8320

Contents lists available at ScienceDirect

Journal of Computational Physics

journal homepage: www.elsevier.com/locate/jcp

A bubble-stabilized least-squares finite element method for steady MHD duct flow problems at high Hartmann numbers

Po-Wen Hsieh, Suh-Yuh Yang *

Department of Mathematics, National Central University, No. 300, Jhongda Road, Jhongli City 32001, Taiwan

ARTICLE INFO

Article history:
Received 3 March 2009
Received in revised form 28 July 2009
Accepted 8 August 2009
Available online 19 August 2009

MSC:
65N12
65N30
76W05

Keywords:
Magnetohydrodynamic equations
Hartmann numbers
Convection-dominated problems
Finite element methods
Residual-free bubbles
Least-squares

ABSTRACT

In this paper we devise a stabilized least-squares finite element method using the residual-free bubbles for solving the governing equations of steady magnetohydrodynamic duct flow. We convert the original system of second-order partial differential equations into a first-order system formulation by introducing two additional variables. Then the least-squares finite element method using C^0 linear elements enriched with the residual-free bubble functions for all unknowns is applied to obtain approximations to the first-order system. The most advantageous features of this approach are that the resulting linear system is symmetric and positive definite, and it is capable of resolving high gradients near the layer regions without refining the mesh. Thus, this approach is possible to obtain approximations consistent with the physical configuration of the problem even for high values of the Hartmann number. Before incoorperating the bubble functions into the global problem, we apply the Galerkin least-squares method to approximate the bubble functions that are exact solutions of the corresponding local problems on elements. Therefore, we indeed introduce a two-level finite element method consisting of a mesh for discretization and a submesh for approximating the computations of the residual-free bubble functions. Numerical results confirming theoretical findings are presented for several examples including the Shercliff problem.

1. Introduction

The purpose of this paper is to devise a stabilized least-squares finite element method using the residual-free bubble functions for solving the magnetohydrodynamic (henceforth, MHD) duct flow problems. It is known that the problem of the flow of viscous, incompressible, electrically conducting fluids in channels and ducts under a uniform oblique magnetic field has many industrial applications in the field of magnetohydrodynamics. Therefore, it is an important research topic to provide an effective numerical method for solving such duct flow problems for the sake of application.

There are many researches which use various numerical methods such as finite difference, finite element, and boundary element methods for the MHD duct flow problems. We refer the reader to [21,22,24–26] and many references cited therein. However, when the Hartmann number is large, such MHD duct flow problem is convection-dominated. It is well-known that the solutions of convection-dominated problems can exhibit localized phenomena such as boundary and interior layers, i.e., narrow regions where the derivative of solution is very large. Therefore, most conventional numerical methods can not efficiently solve the problem because they are lacking in either stability or accuracy. It was pointed out in [21,22] that the common deficiency of the existing numerical methods for the MHD duct flow problem is that they produce physical numerical results in several configurations of interest but the Hartmann number M cannot be increased more than about

* Corresponding author. Tel.: +886 3 4227151x65130; fax: +886 3 4257379.
E-mail addresses: 952401001@cc.ncu.edu.tw (P.-W. Hsieh), syyang@math.ncu.edu.tw (S.-Y. Yang).

0021-9991/$ - see front matter © 2009 Elsevier Inc. All rights reserved.
doi:10.1016/j.jcp.2009.08.007

10^2. However, from a practical point of view, the important range of the Hartmann number in industrial applications is $10^2 \leqslant M \leqslant 10^6$.

One of the most successful class of methods for treating the convection-dominated problems is the stabilized finite element methods. The subject of stabilized finite element methods has been intensively studied for more than twenty years and it is still attractive today. See [12,18], a recent review by Franca et al. [15] and many references cited therein. In particular, the residual-free bubble method which is a stabilized-like finite element method has been demonstrated to be efficient for convection-dominated problems. Recently, Nesliturk and Tezer-Sezgin [21,22] showed that the stabilized finite element method using the residual-free bubbles seems robust in MHD duct flow problems at high Hartmann numbers.

The residual-free bubble method is formulated by enriching the standard C^0 linear finite element space with some specific bubble functions (see, e.g. [4–6,13]). Partitioning the domain into a mesh of elements, the residual-free bubble functions are defined to be as rich as possible within an element. In other words, the bubble functions are required to satisfy some corresponding local equation in the interior of each element, up to the contribution of the linear part, with a homogeneous Dirichlet condition on the element boundary. However, an apparent disadvantage of this approach for convection-dominated convection–diffusion problems is that the resulting linear system is not symmetric. Thus, some efficient and robust solvers for linear systems such as the conjugate gradient method can not be applied.

On the other hand, for the past two decades, least-squares finite element methods (henceforth, LSFEMs) have become more and more frequently used to approximate the solution of first-order system of partial differential equations arising from fluid and solid mechanics. We refer the reader to [1,2,7,9–11,19,23] and many references therein. It is already known that the most specific features of the least-squares finite element approach which give it advantages are that the resulting linear system is symmetric and positive definite, and simple equal low-order finite elements such as the continuous linear elements can be used for the approximation of all unknowns. Unfortunately, it is also known that the primitive LSFEM is not able to achieve good performance for convection-dominated problems.

In the present paper, we will devise a novel least-squares finite element method stabilized with the residual-free bubble functions for approximating the solution of the MHD duct flow problem, which is reformulated as a first-order system by introducing two additional variables. The most distinguished features of this approach are that the resulting linear system is symmetric and positive definite, and this approach is capable of resolving high gradients near the layer regions without refining the mesh. Before incooperating the bubble functions into the global problem, we will apply the Galerkin least-squares method [12,18] to approximate the bubble functions that are analytic solutions of the corresponding local problems on elements. Therefore, we indeed introduce a two-level finite element method consisting of a mesh for discretization and a submesh for approximating the computations of the residual-free bubbles (cf. [13]). We will show that this approach gives more accurate and stable results even for high values of Hartmann number. Numerical results confirming theoretical findings are presented for several examples including the Shercliff problem which possesses an analytic solution.

Now let us remark that the stabilized LSFEM using the residual-free bubbles has been applied to solve the 1-D single convection–diffusion equation in the recent thesis of Kao [20]. Indeed, the basic idea in the work of [20] was initially suggested by the second author of this paper. However a mathematical derivation of the bubble equation (cf. Section 4) corresponding to the additional variable $p := u'$ is lacking therein and hence the present work is aimed at meeting this need. We also extend this bubble-stabilized least-squares approach to the coupled convection-dominated problems in higher dimensions. Moreover, based on our theoretical analysis and simulation results, we find that for achieving higher accuracy and stability, it is more appropriate to replace the additional variable $p := u'$ introduced in [20] by $p := \kappa u'$ (cf. Section 2).

The remainder of this paper is organized as follows. We derive the first-order system formulation for the MHD duct flow problem in Section 2. In Section 3, we introduce the primitive LSFEM, where the continuity and coercivity estimates of the method are established. The bubble-stabilized LSFEM is devised in Section 4 and the construction of residual-free bubble functions is also reported therein. Numerical examples are given in Section 5 to demonstrate the effectiveness of the proposed bubble-stabilized LSFEM. Finally, in Section 6, some conclusions are made.

2. Problem formulation

We study the problem of finding the velocity u and the induced magnetic field b for a laminar, fully developed flow of an incompressible, viscous, electrically conducting fluid in a straight channel with uniform cross-section Ω. The fluid is driven by a constant mechanical pressure gradient $-dp/dz$. The direction of the constant transverse external magnetic field b_0 may be arbitrary to the x-axis, and the fields u and b are parallel to the z-axis. We assume that the cross-section Ω is an open bounded region in $\mathbb{R}^2$ with Lipschitz boundary $\partial\Omega$.

The generalized governing equations for the above duct flow in dimensionless form with suitable boundary conditions can be posed as follows [21,22,24]:

$$\begin{cases} -\kappa\Delta u + \boldsymbol{a}\cdot\nabla b = f \quad \text{in } \Omega, \\ -\kappa\Delta b + \boldsymbol{a}\cdot\nabla u = g \quad \text{in } \Omega, \\ u = 0 \quad \text{on } \partial\Omega, \\ b = 0 \quad \text{on } \Gamma_D, \\ \nabla b\cdot\boldsymbol{n} = 0 \quad \text{on } \Gamma_N, \end{cases} \tag{2.1}$$

where the symbols Δ and ∇ stand for the Laplacian and gradient operators, respectively; $u = u(x,y)$ and $b = b(x,y)$ are the velocity and the induced magnetic field in the z-direction, respectively; $0 < \kappa := 1/M < 1$ is the diffusivity coefficient and $M = b_0 l(\delta/\mu)^{1/2}$ is the Hartmann number, where b_0 is the intensity of the external magnetic field, l is the characteristic length of the duct, δ and μ are the electric conductivity and coefficient of viscosity of the fluid respectively, and in industrial applications one typically has $10^2 \leqslant M \leqslant 10^6$; $\boldsymbol{a} = (-\sin\alpha, -\cos\alpha)^\top$, α is the angle between the externally applied magnetic field b_0 and the x-axis; $f : \Omega \to \mathbb{R}$ and $g : \Omega \to \mathbb{R}$ are given source terms; $\partial\Omega = \Gamma_D \cup \Gamma_N$, where Γ_D has a positive measure and $\Gamma_D \cap \Gamma_N = \varnothing$; $\boldsymbol{n}$ is the outward unit normal vector to $\partial\Omega$.

In order to apply the least-squares finite element method to approximate the solution of problem (2.1), we have to convert problem (2.1) into a first-order system formulation. Introducing two additional variables $\boldsymbol{\omega}$ and $\mathbf{J}$ by

$$\begin{aligned} &\boldsymbol{\omega} = -\kappa\nabla u \quad \text{on } \overline{\Omega},\\ &\mathbf{J} = -\kappa\nabla b \quad \text{on } \overline{\Omega}, \end{aligned}$$

we can transform the problem (2.1) into the following form:

$$\begin{cases} \nabla\cdot\boldsymbol{\omega} + \boldsymbol{a}\cdot\nabla b = f \quad \text{in } \Omega,\\ \nabla\cdot\mathbf{J} + \boldsymbol{a}\cdot\nabla u = g \quad \text{in } \Omega,\\ \boldsymbol{\omega} + \kappa\nabla u = 0 \quad \text{in } \Omega,\\ \mathbf{J} + \kappa\nabla b = 0 \quad \text{in } \Omega,\\ u = 0 \quad \text{on } \partial\Omega,\\ b = 0 \quad \text{on } \Gamma_D,\\ \mathbf{J}\cdot\boldsymbol{n} = 0 \quad \text{on } \Gamma_N. \end{cases} \tag{2.2}$$

Before we go further, we need to introduce some function spaces. Throughout this paper, we will use standard notation and definitions for the Sobolev spaces $H^m(\Omega)$ for nonnegative integers m (cf. [3,16]). The associated inner product and norm are denoted by $(\cdot,\cdot)_m$ and $\|\cdot\|_m$, respectively. As usual, $L^2(\Omega) = H^0(\Omega)$ and $H_0^1(\Omega) = \{v \in H^1(\Omega) \text{ and } v|_{\partial\Omega} = 0\}$. We need the Hilbert space

$$\mathbf{H}(\mathrm{div};\Omega) = \{\mathbf{q} \in (L^2(\Omega))^2 \text{ and } \nabla\cdot\mathbf{q} \in L^2(\Omega)\}$$

with the following inner product and norm: for $\mathbf{p}, \mathbf{q} \in \mathbf{H}(\mathrm{div};\Omega)$,

$$\begin{aligned} &(\mathbf{p},\mathbf{q})_{\mathrm{div}} := (\mathbf{p},\mathbf{q})_0 + (\nabla\cdot\mathbf{p}, \nabla\cdot\mathbf{q})_0,\\ &\|\mathbf{q}\|_{\mathrm{div}} := \left(\|\mathbf{q}\|_0^2 + \|\nabla\cdot\mathbf{q}\|_0^2\right)^{1/2}. \end{aligned}$$

In the analysis of the developed method, we will frequently use the following Green formula:

$$(\mathbf{q}, \nabla v)_0 + (\nabla\cdot\mathbf{q}, v)_0 = (\mathbf{q}\cdot\mathbf{n}, v)_{0,\partial\Omega}, \quad \forall\ \mathbf{q} \in \mathbf{H}(\mathrm{div};\Omega) \text{ and } v \in H^1(\Omega). \tag{2.3}$$

As a consequence of the Green formula (2.3), for $v \in H_0^1(\Omega)$ and $c \in H^1(\Omega)$, we have

$$(\boldsymbol{a}\cdot\nabla c, v)_0 = (\nabla c, v\boldsymbol{a})_0 = (v\boldsymbol{a}\cdot\boldsymbol{n}, c)_{0,\partial\Omega} - (\nabla\cdot(v\boldsymbol{a}), c)_0 = -(\nabla\cdot(v\boldsymbol{a}), c)_0 = -(\boldsymbol{a}\cdot\nabla v, c)_0. \tag{2.4}$$

We also need the following Poincaré–Friedrichs inequality [16]: there exists a constant $C_{pf} > 0$ such that

$$\|v\|_0 \leqslant C_{pf}\|\nabla v\|_0, \quad \forall\ v \in H^1(\Omega) \text{ and } v = 0 \text{ on } \Gamma_D. \tag{2.5}$$

3. The primitive least-squares finite element method

We first define the following four function spaces with respect to the four unknown variables $(u, b, \boldsymbol{\omega}, \mathbf{J})$ of the boundary value problem (2.2):

$$\begin{cases} \mathcal{V} = H_0^1(\Omega),\\ \mathcal{C} = \{c :\ c \in H^1(\Omega) \text{ and } c = 0 \text{ on } \Gamma_D\},\\ \mathcal{W} = \mathbf{H}(\mathrm{div};\Omega),\\ \mathcal{K} = \{\mathbf{K} :\ \mathbf{K} \in \mathbf{H}(\mathrm{div};\Omega) \text{ and } \mathbf{K}\cdot\boldsymbol{n} = 0 \text{ on } \Gamma_N\}. \end{cases} \tag{3.1}$$

Then define the L^2 least-squares energy functional $\mathcal{F} : \mathcal{V}\times\mathcal{C}\times\mathcal{W}\times\mathcal{K} \to \mathbb{R}$ for the extended first-order problem (2.2) by

$$\mathcal{F}((v,c,\boldsymbol{\varphi},\mathbf{K});(f,g)) = \|\nabla\cdot\boldsymbol{\varphi} + \boldsymbol{a}\cdot\nabla c - f\|_0^2 + \|\nabla\cdot\mathbf{K} + \boldsymbol{a}\cdot\nabla v - g\|_0^2 + \|\boldsymbol{\varphi} + \kappa\nabla v - 0\|_0^2 + \|\mathbf{K} + \kappa\nabla c - 0\|_0^2. \tag{3.2}$$

The energy functional $\mathcal{F}(\cdot;(f,g))$ is defined to be the sum of the square L^2-norms of the residuals on the product function space $\mathcal{V}\times\mathcal{C}\times\mathcal{W}\times\mathcal{K}$. Thus, if $(u,b,\boldsymbol{\omega},\mathbf{J}) \in \mathcal{V}\times\mathcal{C}\times\mathcal{W}\times\mathcal{K}$ is an exact solution of problem (2.2), then $(u,b,\boldsymbol{\omega},\mathbf{J})$ must be a zero minimizer of the functional on $\mathcal{V}\times\mathcal{C}\times\mathcal{W}\times\mathcal{K}$, namely,

$$\mathcal{F}((u,b,\boldsymbol{\omega},\mathbf{J});(f,g)) = 0 = \min\{\mathcal{F}((v,c,\boldsymbol{\varphi},\mathbf{K});(f,g)) :\ (v,c,\boldsymbol{\varphi},\mathbf{K}) \in \mathcal{V}\times\mathcal{C}\times\mathcal{W}\times\mathcal{K}\}.$$

Moreover, one can observe that for any given $(v,c,\boldsymbol{\varphi},\mathbf{K}) \in \mathcal{V}\times\mathcal{C}\times\mathcal{W}\times\mathcal{K}$, $\mathcal{F}((u,b,\boldsymbol{\omega},\mathbf{J})+\varepsilon(v,c,\boldsymbol{\varphi},\mathbf{K});(f,g))$ is a nonnegative quadratic functional in the variable $\varepsilon\in\mathbb{R}$. Therefore, we have

$$\frac{d}{d\varepsilon}\mathcal{F}((u,b,\boldsymbol{\omega},\mathbf{J})+\varepsilon(v,c,\boldsymbol{\varphi},\mathbf{K});(f,g))|_{\varepsilon=0}=0$$

which is equivalent to

$$B((u,b,\boldsymbol{\omega},\mathbf{J}),(v,c,\boldsymbol{\varphi},\mathbf{K}))=L((v,c,\boldsymbol{\varphi},\mathbf{K})),\quad \forall\ (v,c,\boldsymbol{\varphi},\mathbf{K})\in\mathcal{V}\times\mathcal{C}\times\mathcal{W}\times\mathcal{K}, \tag{3.3}$$

where the bilinear form $B(\cdot,\cdot)$ and the linear form $L(\cdot)$ are respectively defined as follows:

$$\begin{aligned}B((u,b,\boldsymbol{\omega},\mathbf{J}),(v,c,\boldsymbol{\varphi},\mathbf{K})) &= \int_\Omega (\nabla\cdot\boldsymbol{\omega}+\boldsymbol{a}\cdot\nabla b)(\nabla\cdot\boldsymbol{\varphi}+\boldsymbol{a}\cdot\nabla c)+(\nabla\cdot\mathbf{J}+\boldsymbol{a}\cdot\nabla u)(\nabla\cdot\mathbf{K}+\boldsymbol{a}\cdot\nabla v)\\ &\quad+(\boldsymbol{\omega}+\kappa\nabla u)\cdot(\boldsymbol{\varphi}+\kappa\nabla v)+(\mathbf{J}+\kappa\nabla b)\cdot(\mathbf{K}+\kappa\nabla c)\ d\Omega,\\ L((v,c,\boldsymbol{\varphi},\mathbf{K})) &= \int_\Omega f(\nabla\cdot\boldsymbol{\varphi}+\boldsymbol{a}\cdot\nabla c)+g(\nabla\cdot\mathbf{K}+\boldsymbol{a}\cdot\nabla v)\ d\Omega.\end{aligned}$$

We now consider the finite element formulation of the least-squares method (3.3) for problem (2.2). Let $\mathcal{V}_h\subseteq\mathcal{V},\mathcal{C}_h\subseteq\mathcal{C},\mathcal{W}_h\subseteq\mathcal{W}$, and $\mathcal{K}_h\subseteq\mathcal{K}$ be the standard finite element spaces consisting of continuous piecewise polynomials with degree less or equal than r over a regular triangulation $\mathcal{T}_h$ of the domain Ω. We denote by h_T the diameter of element $T\in\mathcal{T}_h$ and set $h:=\max_{T\in\mathcal{T}_h}h_T$. The primitive LSFEM for problem (2.2) is then defined to be the following problem:

Seek $(u_h,b_h,\boldsymbol{\omega}_h,\mathbf{J}_h)\in\mathcal{V}_h\times\mathcal{C}_h\times\mathcal{W}_h\times\mathcal{K}_h$ such that

$$B((u_h,b_h,\boldsymbol{\omega}_h,\mathbf{J}_h);(v_h,c_h,\boldsymbol{\varphi}_h,\mathbf{K}_h))=L(v_h,c_h,\boldsymbol{\varphi}_h,\mathbf{K}_h), \tag{3.4}$$

for all $(v_h,c_h,\boldsymbol{\varphi}_h,\mathbf{K}_h)\in\mathcal{V}_h\times\mathcal{C}_h\times\mathcal{W}_h\times\mathcal{K}_h$.

Once the basis functions of the finite-dimensional space $\mathcal{V}_h\times\mathcal{C}_h\times\mathcal{W}_h\times\mathcal{K}_h$ are chosen, problem (3.4) is equivalent to solve a linear system problem, $\mathbf{A}\boldsymbol{\xi}=\mathbf{b}$, where unknown vector $\boldsymbol{\xi}$ consists the coordinates of the least-squares finite element solution $(u_h,b_h,\boldsymbol{\omega}_h,\mathbf{J}_h)$ with respect to the chosen basis functions.

The unique solvability of problem (3.4) and error estimates of the least-squares finite element solution $(u_h,b_h,\boldsymbol{\omega}_h,\mathbf{J}_h)$ mainly depend on the continuity and coercivity estimates of the bilinear form B. Before we derive the estimates, we remark that

$$B((v,c,\boldsymbol{\varphi},\mathbf{K});(v,c,\boldsymbol{\varphi},\mathbf{K}))=\mathcal{F}((v,c,\boldsymbol{\varphi},\mathbf{K});\mathbf{0}),\quad\forall\ (v,c,\boldsymbol{\varphi},\mathbf{K})\in\mathcal{V}\times\mathcal{C}\times\mathcal{W}\times\mathcal{K}. \tag{3.5}$$

Theorem 3.1. *Consider the homogeneous L^2 least-squares energy functional $\mathcal{F}(\cdot;\mathbf{0})$ over the product space $\mathcal{V}\times\mathcal{C}\times\mathcal{W}\times\mathcal{K}$. Then there exist two positive constants C_1 and C_2 both independent of κ such that for any $(v,c,\boldsymbol{\varphi},\mathbf{K})\in\mathcal{V}\times\mathcal{C}\times\mathcal{W}\times\mathcal{K}$ we have*

$$\mathcal{F}((v,c,\boldsymbol{\varphi},\mathbf{K});\mathbf{0})\leqslant C_1\Big(\|v\|_1^2+\|c\|_1^2+\|\boldsymbol{\varphi}\|_{\mathrm{div}}^2+\|\mathbf{K}\|_{\mathrm{div}}^2\Big), \tag{3.6}$$

$$\mathcal{F}((v,c,\boldsymbol{\varphi},\mathbf{K});\mathbf{0})\geqslant C_2\kappa^2\Big(\|v\|_1^2+\|c\|_1^2+\|\boldsymbol{\varphi}\|_{\mathrm{div}}^2+\|\mathbf{K}\|_{\mathrm{div}}^2\Big). \tag{3.7}$$

Proof. The continuity estimate (3.6) follows directly from the triangle inequality. We will show the validity of coercivity estimate (3.7). Let α be a positive parameter that will be determined later. Utilizing 2.3, 2.4 and 2.5, we have

$$\begin{aligned}\mathcal{F}((v,c,\boldsymbol{\varphi},\mathbf{K});\mathbf{0}) &= \|\nabla\cdot\boldsymbol{\varphi}+\boldsymbol{a}\cdot\nabla c-\alpha v\|_0^2+2\alpha(\nabla\cdot\boldsymbol{\varphi}+\boldsymbol{a}\cdot\nabla c,v)_0-\alpha^2\|v\|_0^2+\|\nabla\cdot\mathbf{K}+\boldsymbol{a}\cdot\nabla v-\alpha c\|_0^2\\ &\quad+2\alpha(\nabla\cdot\mathbf{K}+\boldsymbol{a}\cdot\nabla v,c)_0-\alpha^2\|c\|_0^2+\|\boldsymbol{\varphi}+\kappa\nabla v-\alpha\nabla v\|_0^2+2\alpha(\boldsymbol{\varphi}+\kappa\nabla v,\nabla v)_0\\ &\quad-\alpha^2\|\nabla v\|_0^2+\|\mathbf{K}+\kappa\nabla c-\alpha\nabla c\|_0^2+2\alpha(\mathbf{K}+\kappa\nabla c,\nabla c)_0-\alpha^2\|\nabla c\|_0^2\\ &\geqslant 2\alpha(\nabla\cdot\boldsymbol{\varphi}+\boldsymbol{a}\cdot\nabla c,v)_0-\alpha^2\|v\|_0^2+2\alpha(\nabla\cdot\mathbf{K}+\boldsymbol{a}\cdot\nabla v,c)_0-\alpha^2\|c\|_0^2\\ &\quad+2\alpha(\boldsymbol{\varphi}+\kappa\nabla v,\nabla v)_0-\alpha^2\|\nabla v\|_0^2+2\alpha(\mathbf{K}+\kappa\nabla c,\nabla c)_0-\alpha^2\|\nabla c\|_0^2\\ &= -\alpha^2\|v\|_0^2-\alpha^2\|c\|_0^2+2\alpha\kappa\|\nabla v\|_0^2-\alpha^2\|\nabla v\|_0^2+2\alpha\kappa\|\nabla c\|_0^2-\alpha^2\|\nabla c\|_0^2\\ &\geqslant \alpha\Big(2\kappa-\alpha\Big(1+C_{pf}^2\Big)\Big)\Big(\|\nabla v\|_0^2+\|\nabla c\|_0^2\Big).\end{aligned}$$

Taking $\alpha=\kappa/\Big(1+C_{pf}^2\Big)<1$, we obtain

$$\mathcal{F}((v,c,\boldsymbol{\varphi},\mathbf{K});\mathbf{0})\geqslant\frac{\kappa^2}{1+C_{pf}^2}\Big(\|\nabla v\|_0^2+\|\nabla c\|_0^2\Big),$$

which implies

$$\|\nabla v\|_0^2 \leqslant \frac{1+C_{pf}^2}{\kappa^2}\mathcal{F}((v,c,\boldsymbol{\varphi},\mathbf{K});\mathbf{0}),$$
$$\|\nabla c\|_0^2 \leqslant \frac{1+C_{pf}^2}{\kappa^2}\mathcal{F}((v,c,\boldsymbol{\varphi},\mathbf{K});\mathbf{0}).$$

Then, it follows from the Poincaré–Friedrichs inequality (2.5) that

$$\|v\|_1^2 = \|v\|_0^2 + \|\nabla v\|_0^2 \leqslant \left(1+C_{pf}^2\right)\|\nabla v\|_0^2 \leqslant \frac{\left(1+C_{pf}^2\right)^2}{\kappa^2}\mathcal{F}((v,c,\boldsymbol{\varphi},\mathbf{K});\mathbf{0}). \tag{3.8}$$

On the other hand, we have

$$\begin{aligned}\|\boldsymbol{\varphi}\|_{\mathrm{div}}^2 &= \|\boldsymbol{\varphi}\|_0^2 + \|\nabla\cdot\boldsymbol{\varphi}\|_0^2 = \|\boldsymbol{\varphi}+\kappa\nabla v-\kappa\nabla v\|_0^2 + \|\nabla\cdot\boldsymbol{\varphi}+\boldsymbol{a}\cdot\nabla c-\boldsymbol{a}\cdot\nabla c\|_0^2\\ &\leqslant 2\left(\|\boldsymbol{\varphi}+\kappa\nabla v\|_0^2 + \|\kappa\nabla v\|_0^2 + \|\nabla\cdot\boldsymbol{\varphi}+\boldsymbol{a}\cdot\nabla c\|_0^2 + \|\boldsymbol{a}\cdot\nabla c\|_0^2\right)\\ &\leqslant C\left(\mathcal{F}((v,c,\boldsymbol{\varphi},\mathbf{K});\mathbf{0}) + \frac{1}{\kappa^2}\mathcal{F}((v,c,\boldsymbol{\varphi},\mathbf{K});\mathbf{0})\right) \leqslant \frac{2C}{\kappa^2}\mathcal{F}((v,c,\boldsymbol{\varphi},\mathbf{K});\mathbf{0})),\end{aligned} \tag{3.9}$$

where C is some positive constant independent of κ. Applying the same techniques, we can prove that

$$\|c\|_1^2 \leqslant \frac{\left(1+C_{pf}^2\right)^2}{\kappa^2}\mathcal{F}((v,c,\boldsymbol{\varphi},\mathbf{K});\mathbf{0}), \tag{3.10}$$
$$\|\mathbf{K}\|_{\mathrm{div}}^2 \leqslant \frac{2C}{\kappa^2}\mathcal{F}((v,c,\boldsymbol{\varphi},\mathbf{K});\mathbf{0}). \tag{3.11}$$

Finally, combining (3.8)–(3.10) and (3.11) we obtain (3.7). This completes the proof. □

Based on the coercivity estimate (3.7) of the bilinear form B, one can easily verify that the matrix $\mathbf{A}$ of the linear system $\mathbf{A}\boldsymbol{\xi}=\mathbf{b}$ is symmetric and positive definite, which implies that problem (3.4) has a unique solution. We refer the reader to [19] for more details. Furthermore, we have the following error estimate for the least-squares finite element solution $(u_h,b_h,\boldsymbol{\omega}_h,\mathbf{J}_h)$:

Theorem 3.2. *Assume that $(u,b,\boldsymbol{\omega},\mathbf{J}) \in (\mathcal{V}\times\mathcal{C}\times\mathcal{W}\times\mathcal{K})\cap(H^{r+1}(\Omega))^6$ is the exact solution of problem (2.2). Then the least-squares finite element solution $(u_h,b_h,\boldsymbol{\omega}_h,\mathbf{J}_h)\in\mathcal{V}_h\times\mathcal{C}_h\times\mathcal{W}_h\times\mathcal{K}_h$ satisfies the following estimate:*

$$\kappa(\|u-u_h\|_1 + \|b-b_h\|_1 + \|\boldsymbol{\omega}-\boldsymbol{\omega}_h\|_{\mathrm{div}} + \|\mathbf{J}-\mathbf{J}_h\|_{\mathrm{div}}) \leqslant Ch^r(\|u\|_{r+1} + \|b\|_{r+1} + \|\boldsymbol{\omega}\|_{r+1} + \|\mathbf{J}\|_{r+1}), \tag{3.12}$$

where C is a positive constant independent of κ and h.

Proof. Let $u_I\in\mathcal{V}_h, b_I\in\mathcal{C}_h, \boldsymbol{\omega}_I\in\mathcal{W}_h$ and $\mathbf{J}_I\in\mathcal{K}_h$ be the interpolants of $u, b, \boldsymbol{\omega}$ and $\mathbf{J}$, respectively. Then from the approximation theory, we have

$$\begin{cases}\|u-u_I\|_1 \leqslant Ch^r\|u\|_{r+1},\\ \|b-b_I\|_1 \leqslant Ch^r\|b\|_{r+1},\\ \|\boldsymbol{\omega}-\boldsymbol{\omega}_I\|_{\mathrm{div}} \leqslant Ch^r\|\boldsymbol{\omega}\|_{r+1},\\ \|\mathbf{J}-\mathbf{J}_I\|_{\mathrm{div}} \leqslant Ch^r\|\mathbf{J}\|_{r+1}.\end{cases} \tag{3.13}$$

Now let $U:=(u,b,\boldsymbol{\omega},\mathbf{J}), U_h:=(u_h,b_h,\boldsymbol{\omega}_h,\mathbf{J}_h)$ and $U_I:=(u_I,b_I,\boldsymbol{\omega}_I,\mathbf{J}_I)$. By (3.3) and (3.4), we have the following orthogonality property

$$B(U-U_h,V_h)=0,\quad \forall\, V_h:=(v_h,c_h,\boldsymbol{\varphi}_h,\mathbf{K}_h)\in\mathcal{V}_h\times\mathcal{C}_h\times\mathcal{W}_h\times\mathcal{K}_h.$$

Based on this property with the Cauchy–Schwarz inequality, we obtain

$$B(U-U_h,U-U_h) = B(U-U_h,U-U_I) \leqslant B^{1/2}(U-U_h,U-U_h)B^{1/2}(U-U_I,U-U_I),$$

and then

$$B^{1/2}(U-U_h,U-U_h) \leqslant B^{1/2}(U-U_I,U-U_I). \tag{3.14}$$

Now combining (3.14) with Theorem 3.1 and the approximation properties (3.13) yields the conclusion (3.12). This completes the proof. □

From the error estimate (3.12), we can easily find that when κ is sufficiently small, the primitive LSFEM may perform poorly in practice. This observation has been confirmed by our numerical experiments reported in Section 5. In order to improve the performance of primitive LSFEM, we are going to introduce a bubble-stabilized LSFEM in the next section.

4. A bubble-stabilized least-squares finite element method

In this section, we will introduce a stabilized LSFEM using the residual-free bubble functions to solve the steady MHD duct flow in the first-order system formulation (2.2). We first construct the residual-free bubble functions for the variables u and b. Define the following notation:

$$\mathcal{D} := \begin{bmatrix} -\kappa\Delta & \boldsymbol{a}\cdot\nabla \\ \boldsymbol{a}\cdot\nabla & -\kappa\Delta \end{bmatrix}, \quad \widetilde{U}_h := \begin{bmatrix} u_h \\ b_h \end{bmatrix}, \quad R := \begin{bmatrix} f \\ g \end{bmatrix}.$$

Suppose that the first two components u_h and b_h of stabilized least-squares solution $(u_h, b_h, \boldsymbol{\omega}_h, \mathbf{J}_h)$ have the form $\widetilde{U}_h = \widetilde{U}_1 + \widetilde{U}_b$, where $\widetilde{U}_1$ is the continuous piecewise linear part and $\widetilde{U}_b$ is the bubble part. For each element $T \in \mathcal{T}_h$, we require

$$\begin{cases} \mathcal{D}(\widetilde{U}_1 + \widetilde{U}_b) = R & \text{in } T, \\ \widetilde{U}_b = \mathbf{0} & \text{on } \partial T. \end{cases}$$

We call $\widetilde{U}_b$ a residual-free bubble function on T since $R - \mathcal{D}(\widetilde{U}_1 + \widetilde{U}_b) = \mathbf{0}$ in T and $\widetilde{U}_b|_{\partial T} = \mathbf{0}$. To solve the above problem for $\widetilde{U}_b$, we assume that

$$\widetilde{U}_1 = \sum_{i \in I(u,b)} \alpha_i \Psi_i,$$

where Ψ_i's are the basis functions of $\widetilde{U}_1$ and $I(u,b)$ denotes the associated index set. Then by solving

$$\begin{cases} \mathcal{D}\Phi_{i,T} = -\mathcal{D}\Psi_i & \text{in } T, \\ \Phi_{i,T} = \mathbf{0} & \text{on } \partial T, \end{cases} \tag{4.1}$$

and

$$\begin{cases} \mathcal{D}\Phi_{R,T} = R & \text{in } T, \\ \Phi_{R,T} = \mathbf{0} & \text{on } \partial T, \end{cases} \tag{4.2}$$

for all $T \in \mathcal{T}_h$, we have

$$\widetilde{U}_b = \sum_{i \in I(u,b)} \alpha_i \Phi_i + \Phi_R,$$

which implies that

$$\widetilde{U}_h = \sum_{i \in I(u,b)} \alpha_i (\Psi i + \Phi_i) + \Phi_R, \tag{4.3}$$

where $\Phi_i := \sum_T \Phi_{i,T}$ and $\Phi_R := \sum_T \Phi_{R,T}$.

Next, we construct the residual-free bubbles for the variables $\boldsymbol{\omega}$ and $\mathbf{J}$. Suppose that the solution (u,b) of problem (2.1) is sufficiently smooth. Since

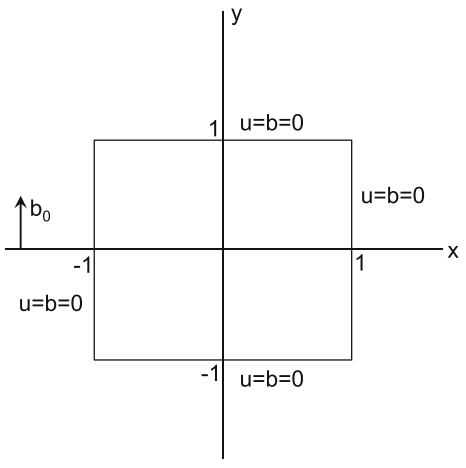

Fig. 5.1. Boundary conditions of the Shercliff problem.

$$\begin{cases} \nabla\cdot\boldsymbol{\omega}+\boldsymbol{a}\cdot\left(-\frac{1}{\kappa}\mathbf{J}\right)=f & \text{in } \Omega,\\ \nabla\cdot\mathbf{J}+\boldsymbol{a}\cdot\left(-\frac{1}{\kappa}\boldsymbol{\omega}\right)=g & \text{in } \Omega, \end{cases}$$

we obtain

$$\begin{cases} \nabla(-\kappa\nabla\cdot\boldsymbol{\omega}+\boldsymbol{a}\cdot\mathbf{J})=-\kappa\nabla f & \text{in } \Omega,\\ \nabla(-\kappa\nabla\cdot\mathbf{J}+\boldsymbol{a}\cdot\boldsymbol{\omega})=-\kappa\nabla g & \text{in } \Omega. \end{cases}$$

Utilizing the fact that $\nabla\times\boldsymbol{\omega}=\nabla\times\mathbf{J}=0$ in Ω, namely,

$$\frac{\partial\omega_2}{\partial x}=\frac{\partial\omega_1}{\partial y}\quad\text{and}\quad\frac{\partial J_2}{\partial x}=\frac{\partial J_1}{\partial y}\quad\text{in }\Omega,$$

we have

$$\begin{cases} -\kappa\Delta\omega_1+\boldsymbol{a}\cdot\nabla J_1=-\kappa\frac{\partial f}{\partial x} & \text{in } \Omega,\\ -\kappa\Delta J_1+\boldsymbol{a}\cdot\nabla\omega_1=-\kappa\frac{\partial g}{\partial x} & \text{in } \Omega; \end{cases}$$
$$\begin{cases} -\kappa\Delta\omega_2+\boldsymbol{a}\cdot\nabla J_2=-\kappa\frac{\partial f}{\partial y} & \text{in } \Omega,\\ -\kappa\Delta J_2+\boldsymbol{a}\cdot\nabla\omega_2=-\kappa\frac{\partial g}{\partial y} & \text{in } \Omega. \end{cases}$$

Define the following notation:

$$\widetilde{W}_h^1:=\begin{bmatrix}\omega_{1h}\\ J_{1h}\end{bmatrix}\quad\text{and}\quad R_x:=\begin{bmatrix}-\kappa\frac{\partial f}{\partial x}\\ -\kappa\frac{\partial g}{\partial x}\end{bmatrix},$$
$$\widetilde{W}_h^2:=\begin{bmatrix}\omega_{2h}\\ J_{2h}\end{bmatrix}\quad\text{and}\quad R_y:=\begin{bmatrix}-\kappa\frac{\partial f}{\partial y}\\ -\kappa\frac{\partial g}{\partial y}\end{bmatrix}.$$

Table 5.1
Least-squares finite element solutions for the Shercliff problem with $\kappa = 1/100$.

Method	x	y	u_h	u_{exact}	b_h	b_{exact}
Primitive LSFEM	0.00	0.00	0.0088870	0.0100000	0.0000000	0.0000000
	0.25	0.00	0.0088869	0.0100000	−0.0024943	−0.0025000
	0.50	0.00	0.0088868	0.0100000	−0.0049886	−0.0050000
	0.75	0.00	0.0088866	0.0100000	−0.0074829	−0.0075000
	0.00	0.25	0.0088832	0.0100000	0.0000000	0.0000000
	0.25	0.25	0.0088836	0.0100000	−0.0024950	−0.0025000
	0.50	0.25	0.0088850	0.0100000	−0.0049901	−0.0050000
	0.75	0.25	0.0088868	0.0099999	−0.0074852	−0.0074999
	0.00	0.50	0.0089074	0.0099992	0.0000000	0.0000000
	0.25	0.50	0.0089062	0.0099981	−0.0024977	−0.0024982
	0.50	0.50	0.0089029	0.0099944	−0.0049916	−0.0049944
	0.75	0.50	0.0088977	0.0099868	−0.0074784	−0.0074868
	0.00	0.75	0.0088933	0.0097614	0.0000000	0.0000000
	0.25	0.75	0.0088468	0.0097163	−0.0022393	−0.0023030
	0.50	0.75	0.0087086	0.0095858	−0.0044826	−0.0046024
	0.75	0.75	0.0084850	0.0093863	−0.0067255	−0.0068869
Stabilized LSFEM	0.00	0.00	0.0096485	0.0100000	0.0000000	0.0000000
	0.25	0.00	0.0096467	0.0100000	−0.0024848	−0.0025000
	0.50	0.00	0.0096414	0.0100000	−0.0049694	−0.0050000
	0.75	0.00	0.0096332	0.0100000	−0.0074538	−0.0075000
	0.00	0.25	0.0096626	0.0100000	0.0000000	0.0000000
	0.25	0.25	0.0096594	0.0100000	−0.0024776	−0.0025000
	0.50	0.25	0.0096500	0.0100000	−0.0049549	−0.0050000
	0.75	0.25	0.0096351	0.0099999	−0.0074318	−0.0074999
	0.00	0.50	0.0096978	0.0099992	0.0000000	0.0000000
	0.25	0.50	0.0096888	0.0099981	−0.0024474	−0.0024982
	0.50	0.50	0.0096616	0.0099944	−0.0048940	−0.0049944
	0.75	0.50	0.0096175	0.0099868	−0.0073393	−0.0074868
	0.00	0.75	0.0092838	0.0097614	0.0000000	0.0000000
	0.25	0.75	0.0092615	0.0097163	−0.0023504	−0.0023030
	0.50	0.75	0.0091937	0.0095858	−0.0046990	−0.0046024
	0.75	0.75	0.0090788	0.0093863	−0.0070441	−0.0068869

Suppose that the components $\widetilde{W}_h^i$ of stabilized least-squares solution $(u_h, b_h, \omega_h, \mathbf{J}_h)$ have the form $\widetilde{W}_h^i = \widetilde{W}_1^i + \widetilde{W}_b^i$ for $i = 1, 2$, where $\widetilde{W}_1^i$ is the linear part and $\widetilde{W}_b^i$ is the bubble part. Similar to the construction of residual-free bubble functions for the variables u and b, we require for each element $T \in \mathcal{T}_h$

$$\begin{cases} \mathcal{D}\left(\widetilde{W}_1^1 + \widetilde{W}_b^1\right) = R_x & \text{in } T, \\ \widetilde{W}_b^1 = \mathbf{0} & \text{on } \partial T, \end{cases}$$

and

Table 5.2
Least-squares finite element solutions for the Shercliff problem with $\kappa = 1/500$.

Method	x	y	u_h	u_{exact}	b_h	b_{exact}
Primitive LSFEM	0.00	0.00	0.0007263	0.0020000	0.0000000	0.0000000
	0.25	0.00	0.0007263	0.0020000	−0.0004976	−0.0005000
	0.50	0.00	0.0007264	0.0020000	−0.0009953	−0.0010000
	0.75	0.00	0.0007263	0.0020000	−0.0014927	−0.0015000
	0.00	0.25	0.0007266	0.0020000	0.0000000	0.0000000
	0.25	0.25	0.0007266	0.0020000	−0.0004976	−0.0005000
	0.50	0.25	0.0007265	0.0020000	−0.0009953	−0.0010000
	0.75	0.25	0.0007264	0.0020000	−0.0014927	−0.0015000
	0.00	0.50	0.0007235	0.0020000	0.0000000	0.0000000
	0.25	0.50	0.0007237	0.0020000	−0.0004988	−0.0005000
	0.50	0.50	0.0007243	0.0020000	−0.0009976	−0.0010000
	0.75	0.50	0.0007251	0.0020000	−0.0014963	−0.0015000
	0.00	0.75	0.0007476	0.0020000	0.0000000	0.0000000
	0.25	0.75	0.0007461	0.0019999	−0.0004883	−0.0004999
	0.50	0.75	0.0007419	0.0019997	−0.0009756	−0.0009997
	0.75	0.75	0.0007356	0.0019992	−0.0014592	−0.0014992
Stabilized LSFEM	0.00	0.00	0.0019588	0.0020000	0.0000000	0.0000000
	0.25	0.00	0.0019584	0.0020000	−0.0004970	−0.0005000
	0.50	0.00	0.0019572	0.0020000	−0.0009941	−0.0010000
	0.75	0.00	0.0019555	0.0020000	−0.0014911	−0.0015000
	0.00	0.25	0.0019590	0.0020000	0.0000000	0.0000000
	0.25	0.25	0.0019585	0.0020000	−0.0004968	−0.0005000
	0.50	0.25	0.0019571	0.0020000	−0.0009936	−0.0010000
	0.75	0.25	0.0019550	0.0020000	−0.0014904	−0.0015000
	0.00	0.50	0.0019599	0.0020000	0.0000000	0.0000000
	0.25	0.50	0.0019592	0.0020000	−0.0004960	−0.0005000
	0.50	0.50	0.0019570	0.0020000	−0.0009920	−0.0010000
	0.75	0.50	0.0019536	0.0020000	−0.0014880	−0.0015000
	0.00	0.75	0.0019623	0.0020000	0.0000000	0.0000000
	0.25	0.75	0.0019612	0.0019999	−0.0004944	−0.0004999
	0.50	0.75	0.0019577	0.0019997	−0.0009888	−0.0009997
	0.75	0.75	0.0019515	0.0019992	−0.0014832	−0.0014992

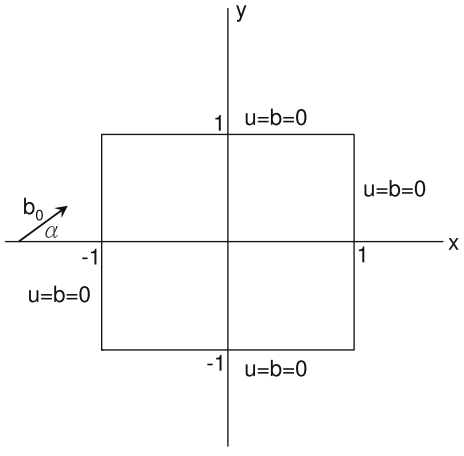

Fig. 5.2. Boundary conditions of Example 5.2.

$$\begin{cases} \mathcal{D}\left(\widetilde{W}_1^2 + \widetilde{W}_b^2\right) = R_y & \text{in } T, \\ \widetilde{W}_b^2 = \mathbf{0} & \text{on } \partial T. \end{cases}$$

Then we can derive from the similar arguments that

$$\widetilde{W}_h^1 = \sum_{i \in I(\omega_1 J_1)} \beta_i(\Psi_i + \Phi_i) + \Phi_{R_x}, \tag{4.4}$$

$$\widetilde{W}_h^2 = \sum_{i \in I(\omega_2 J_2)} \gamma_i(\Psi_i + \Phi_i) + \Phi_{R_y}, \tag{4.5}$$

where $\Phi_{R_x} := \sum_T \Phi_{R_x,T}, \Phi_{R_y} := \sum_T \Phi_{R_y,T}, I(\omega_1, J_1)$ and $I(\omega_2, J_2)$ denote the associated index sets.

Combining (4.3) and (4.4) with (4.5), we conclude that the stabilized least-squares solution can be expressed in the form

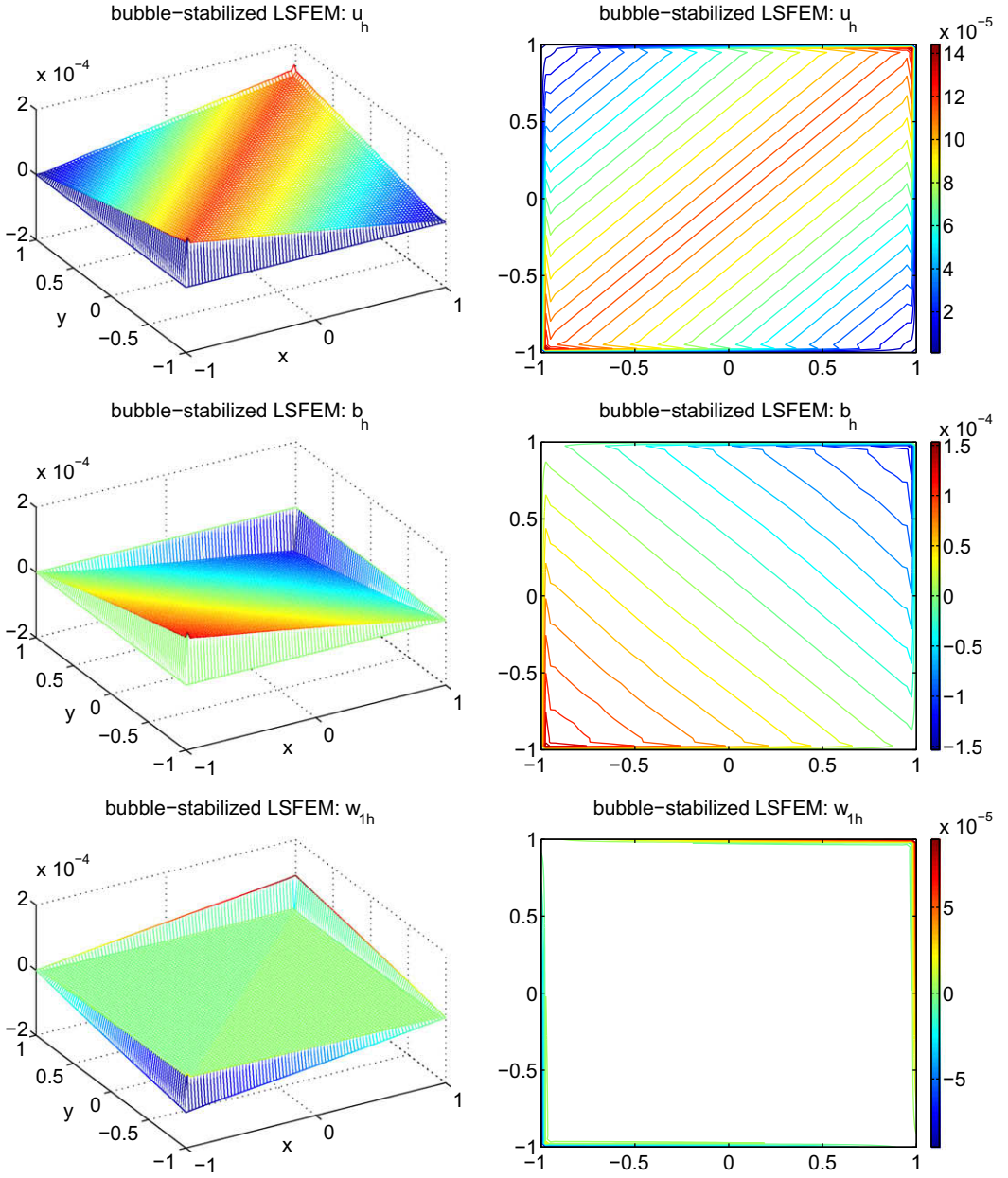

Fig. 5.3. Numerical solutions obtained by the bubble-stabilized LSFEM for Example 5.2 with $\kappa = 10^{-4}$ and $\alpha = \pi/4$.

$$\begin{bmatrix} u_h \\ b_h \\ \omega_{1h} \\ J_{1h} \\ \omega_{2h} \\ J_{2h} \end{bmatrix} = \sum_{i\in I(u,b)} \alpha_i \begin{bmatrix} \Psi_i + \Phi_i \\ \mathbf{0} \\ \mathbf{0} \end{bmatrix} + \sum_{i\in I(\omega_1 J_1)} \beta_i \begin{bmatrix} \mathbf{0} \\ \Psi_i + \Phi_i \\ \mathbf{0} \end{bmatrix} + \sum_{i\in I(\omega_2 J_2)} \gamma_i \begin{bmatrix} \mathbf{0} \\ \mathbf{0} \\ \Psi_i + \Phi_i \end{bmatrix} + \begin{bmatrix} \Phi_R \\ \Phi_{R_x} \\ \Phi_{R_y} \end{bmatrix}.$$

We then define a finite-dimensional space $\mathbf{V}_h$ for the approximate solution $(u_h, b_h, \omega_{1h}, J_{1h}, \omega_{2h}, J_{2h})^\top$ of problem (2.2) by

$$\mathbf{V}_h = \operatorname{span}\left\{ \begin{bmatrix} \Psi_i + \Phi_i \\ \mathbf{0} \\ \mathbf{0} \end{bmatrix}, \begin{bmatrix} \mathbf{0} \\ \Psi_j + \Phi_j \\ \mathbf{0} \end{bmatrix}, \begin{bmatrix} \mathbf{0} \\ \mathbf{0} \\ \Psi_k + \Phi_k \end{bmatrix} : \ i \in I(u,b), j \in I(\omega_1, J_1), k \in I(\omega_2, J_2) \right\}.$$

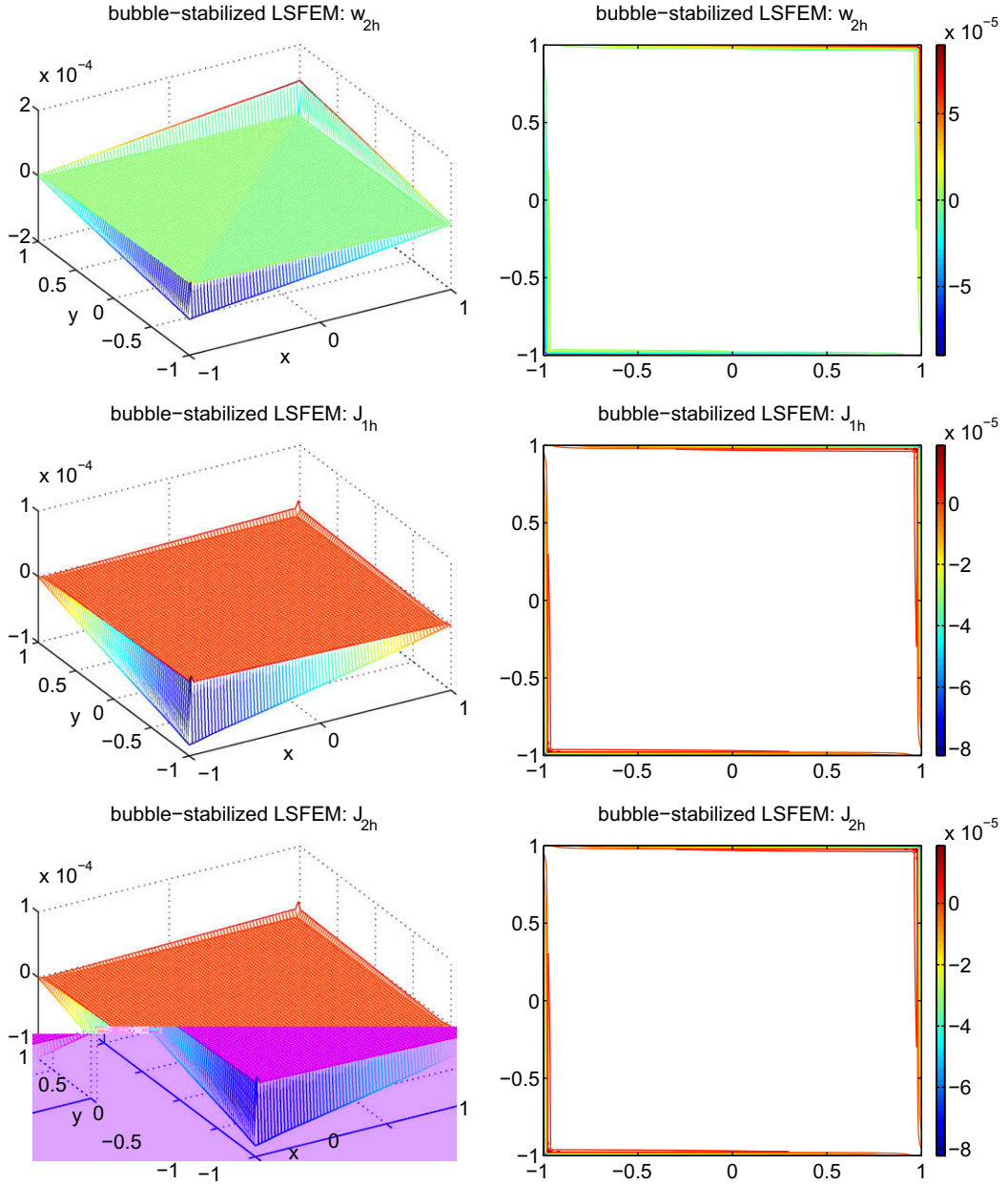

Fig 5.3. *(continued)*

Now we set a permutation function $\mathcal{P}$ by

$$\mathcal{P}((v_1, v_2, v_3, v_4, v_5, v_6)^\top) = (v_1, v_2, v_3, v_5, v_4, v_6)^\top.$$

Then the enriched finite-dimensional space $\widetilde{\mathbf{V}}_h$ for problem (2.2) is defined by

$$\widetilde{\mathbf{V}}_h = \mathcal{P}(\mathbf{V}_h),$$

and the bubble-stabilized LSFEM is defined as the following problem:

Seek $(u_h, b_h, \omega_h, \mathbf{J}_h) := \left(\tilde{u}_h, \tilde{b}_h, \tilde{\omega}_h, \tilde{\mathbf{J}}_h\right) + \mathcal{P}((\Phi_R, \Phi_{R_x}, \Phi_{R_y})^\top)$, where $\left(\tilde{u}_h, \tilde{b}_h, \tilde{\omega}_h, \tilde{\mathbf{J}}_h\right) \in \widetilde{\mathbf{V}}_h$ such that

$$B((u_h, b_h, \omega_h, \mathbf{J}_h); (\tilde{v}_h, \tilde{c}_h, \tilde{\varphi}_h, \widetilde{\mathbf{K}}_h)) = L\left(\tilde{v}_h, \tilde{c}_h, \tilde{\varphi}_h, \widetilde{\mathbf{K}}_h\right), \tag{4.6}$$

for all $\left(\tilde{v}_h, \tilde{c}_h, \tilde{\varphi}_h, \widetilde{\mathbf{K}}_h\right) \in \widetilde{\mathbf{V}}_h$.

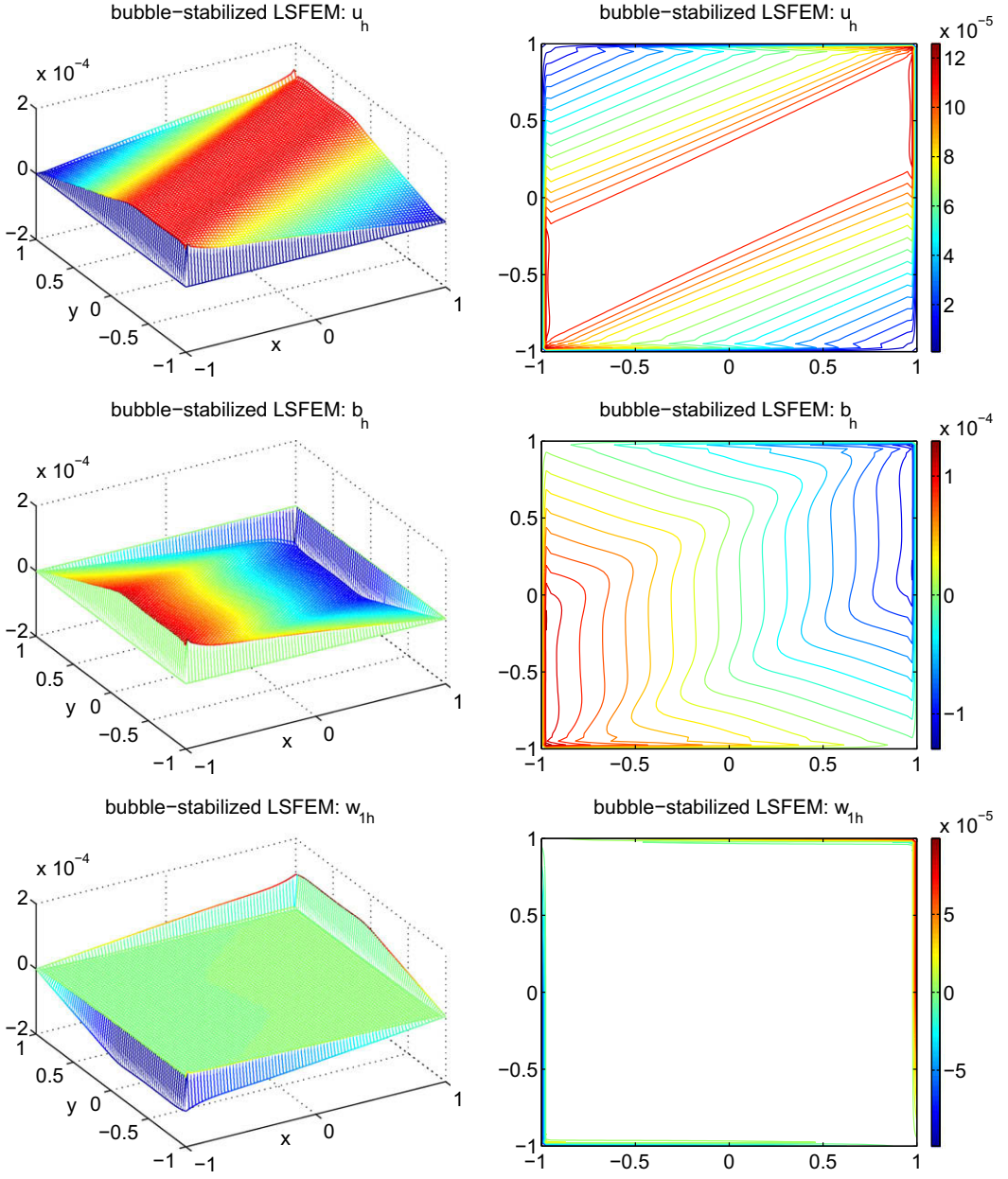

Fig. 5.4. Numerical solutions obtained by the bubble-stabilized LSFEM for Example 5.2 with $\kappa = 10^{-4}$ and $\alpha = \pi/3$.

Again, one can easily verify that problem (4.6) is equivalent to a linear system problem in which the associated matrix is symmetric and positive definite. Consequently, problem (4.6) possesses an unique solution. Moreover, the coercivity estimate (3.7) provides the numerical stability of the bubble-stabilized LSFEM (4.6).

Finally, as an example, we explain some details for resolving the problem (4.1). For

$$\Psi_i = \begin{bmatrix} \psi_i \\ 0 \end{bmatrix} \quad \text{or} \quad \Psi_i = \begin{bmatrix} 0 \\ \psi_i \end{bmatrix}, \quad i \in I(u,b),$$

where ψ_i's are the continuous piecewise linear basis functions, problem (4.1) can be rewritten as follows:

$$\begin{cases} -\kappa\Delta\phi^u_{i,T} + \boldsymbol{a}\cdot\nabla\phi^b_{i,T} = -(-\kappa\Delta\psi_i) & \text{in } T, \\ -\kappa\Delta\phi^b_{i,T} + \boldsymbol{a}\cdot\nabla\phi^u_{i,T} = -(\boldsymbol{a}\cdot\nabla\psi_i) & \text{in } T, \\ \phi^u_{i,T} = \phi^b_{i,T} = 0 & \text{on } \partial T, \end{cases} \tag{4.7}$$

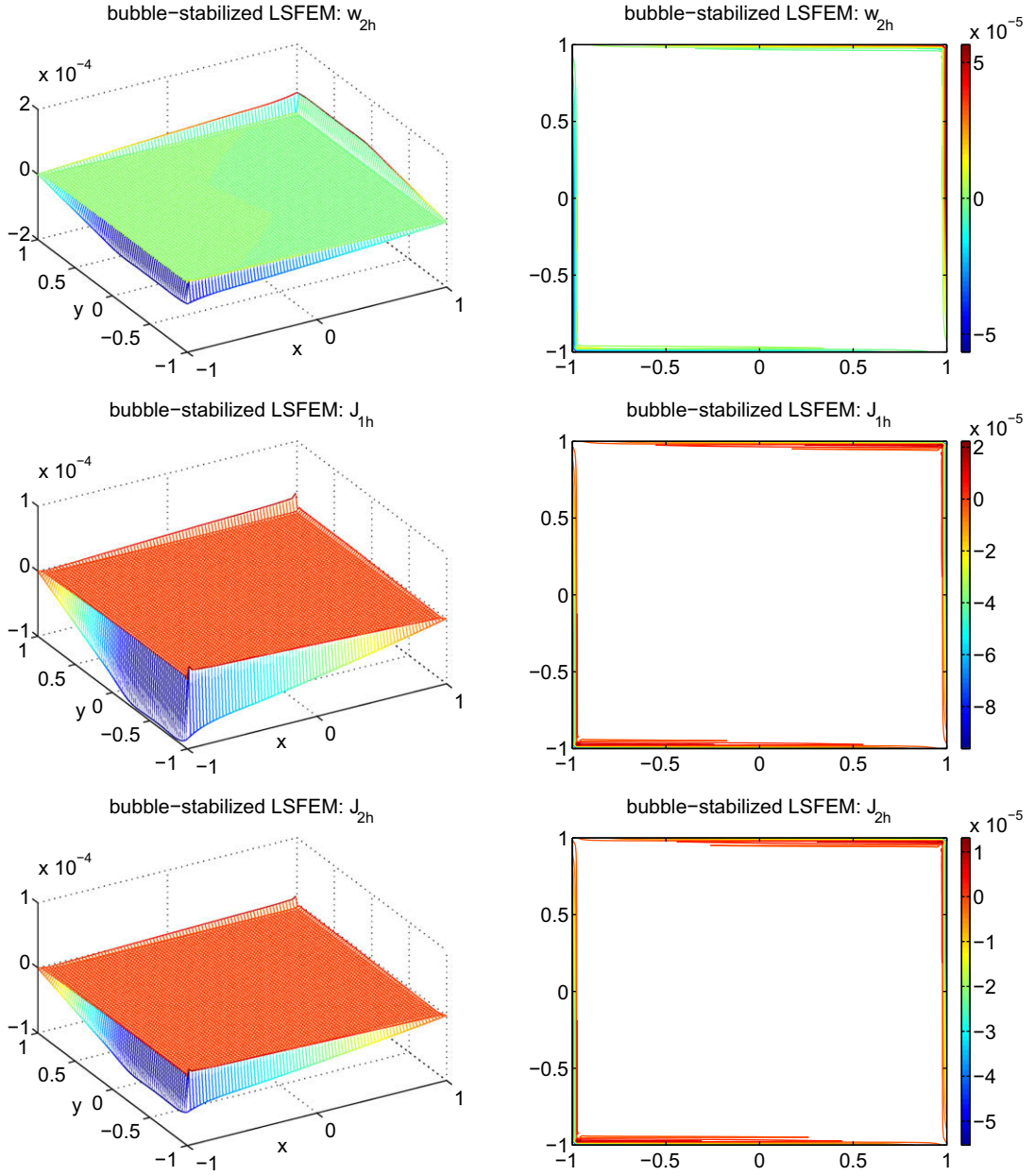

Fig 5.4. *(continued)*

or

$$\begin{cases} -\kappa\Delta\varphi^u_{i,T} + \boldsymbol{a}\cdot\nabla\varphi^b_{i,T} = -(\boldsymbol{a}\cdot\nabla\psi_i) & \text{in } T, \\ -\kappa\Delta\varphi^b_{i,T} + \boldsymbol{a}\cdot\nabla\varphi^u_{i,T} = -(-\kappa\Delta\psi_i) & \text{in } T, \\ \varphi^u_{i,T} = \varphi^b_{i,T} = 0 \quad \text{on } \partial T. \end{cases} \tag{4.8}$$

Now define

$$\breve{S}_{i,T} := \phi^u_{i,T} + \phi^b_{i,T} \quad \text{and} \quad \breve{N}_{i,T} := \phi^u_{i,T} - \phi^b_{i,T},$$
$$S_{i,T} := \varphi^u_{i,T} + \varphi^b_{i,T} \quad \text{and} \quad N_{i,T} := \varphi^u_{i,T} - \varphi^b_{i,T}.$$

Then both problems (4.7) and (4.8) can be decoupled into two single-equation convection-dominated problems:

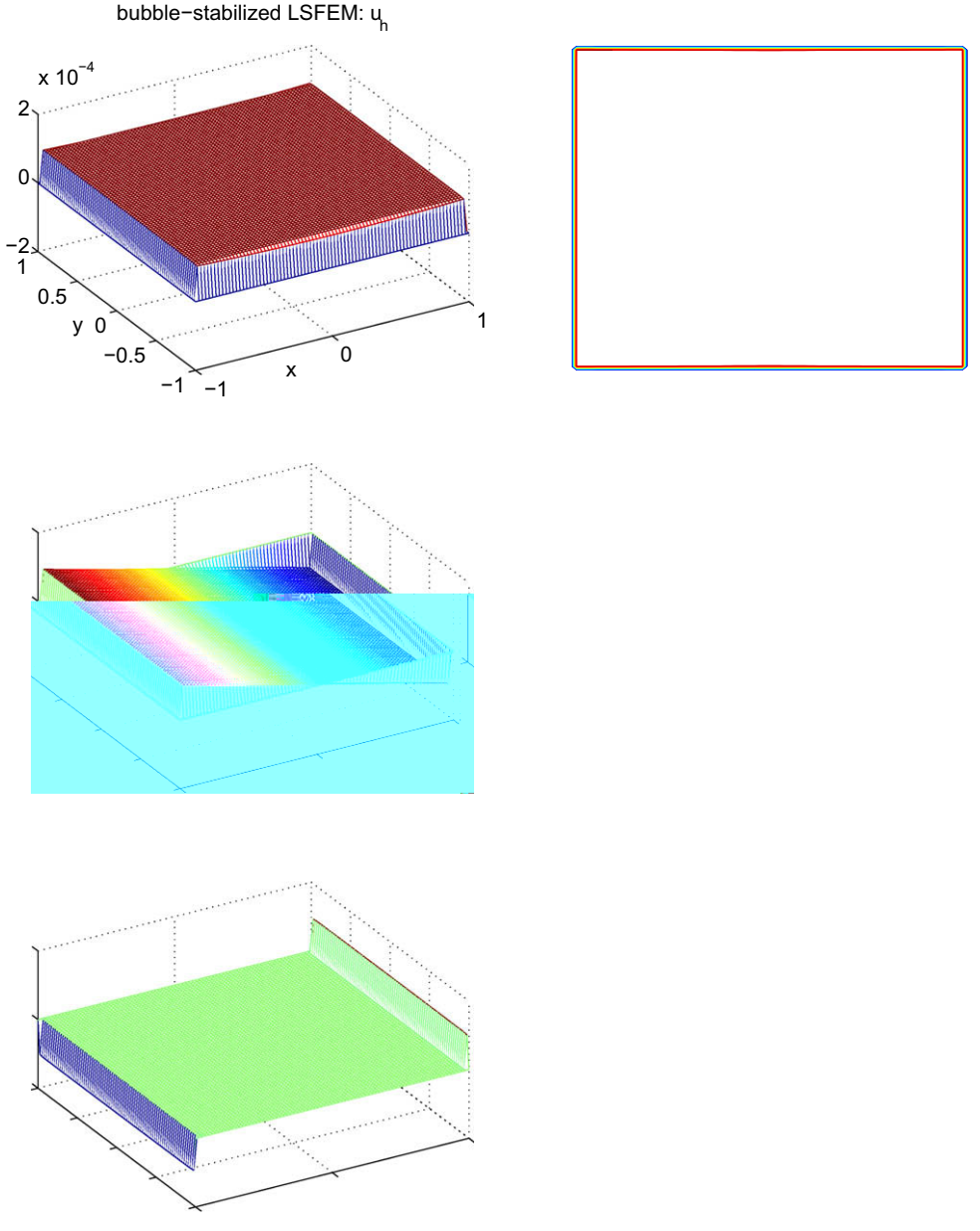

$$\begin{cases} -\kappa\Delta\breve{S}_{i,T} + \boldsymbol{a}\cdot\nabla\breve{S}_{i,T} = -(-\kappa\Delta\psi_i + \boldsymbol{a}\cdot\nabla\psi_i) & \text{in } T, \\ \breve{S}_{i,T} = 0 \quad \text{on } \partial T; \end{cases} \tag{4.9}$$

$$\begin{cases} -\kappa\Delta\breve{N}_{i,T} - \boldsymbol{a}\cdot\nabla\breve{N}_{i,T} = -(-\kappa\Delta\psi_i - \boldsymbol{a}\cdot\nabla\psi_i) & \text{in } T, \\ \breve{N}_{i,T} = 0 \quad \text{on } \partial T; \end{cases} \tag{4.10}$$

and

$$\begin{cases} -\kappa\Delta S_{i,T} + \boldsymbol{a}\cdot\nabla S_{i,T} = -(-\kappa\Delta\psi_i + \boldsymbol{a}\cdot\nabla\psi_i) & \text{in } T, \\ S_{i,T} = 0 \quad \text{on } \partial T; \end{cases} \tag{4.11}$$

$$\begin{cases} -\kappa\Delta N_{i,T} - \boldsymbol{a}\cdot\nabla N_{i,T} = -\kappa\Delta\psi_i - \boldsymbol{a}\cdot\nabla\psi_i & \text{in } T, \\ N_{i,T} = 0 \quad \text{on } \partial T. \end{cases} \tag{4.12}$$

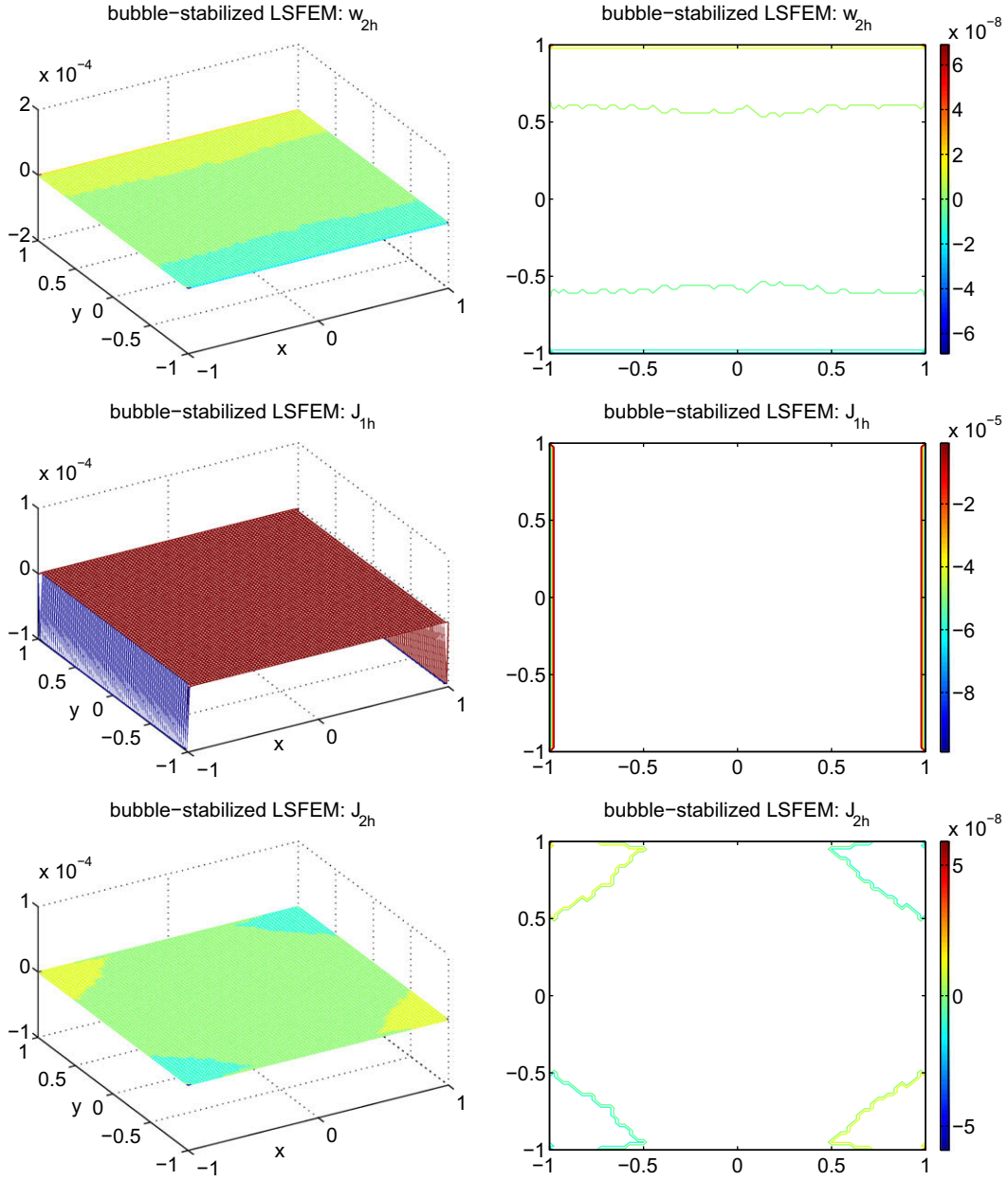

Fig 5.5. *(continued)*

Comparing problems (4.9) with (4.11) and (4.10) with (4.12), one can find that $S_{i,T} = \breve{S}_{i,T}$ and $N_{i,T} = -\breve{N}_{i,T}$. Hence, we have

$$\Phi_{i,T} = \begin{bmatrix} \phi^u_{i,T} \\ \phi^b_{i,T} \end{bmatrix} = \frac{1}{2} \begin{bmatrix} \breve{S}_{i,T} + \breve{N}_{i,T} \\ \breve{S}_{i,T} - \breve{N}_{i,T} \end{bmatrix}$$

or

$$\Phi_{i,T} = \begin{bmatrix} \varphi^u_{i,T} \\ \varphi^b_{i,T} \end{bmatrix} = \frac{1}{2} \begin{bmatrix} \breve{S}_{i,T} - \breve{N}_{i,T} \\ \breve{S}_{i,T} + \breve{N}_{i,T} \end{bmatrix}.$$

Notice that $\Delta\psi_i =$

Example 5.1 (*The Shercliff problem*). This is an example with an analytic solution whose numerical data are available in [21], so that we can compare our numerical results with the exact solution. In this example, the walls of the channel are insulated, i.e., $b = 0$ on $\partial\Omega$, and the velocity is zero on the solid walls, i.e., $u = 0$ on $\partial\Omega$. The external magnetic field is perpendicular to the x-axis ($\alpha = \pi/2$), see Fig. 5.1. The right-hand side source functions in problem (2.2) are given by $f = \kappa$ and $g = 0$.

In Tables 5.1 and 5.2, we compare the approximate solutions generated by the primitive LSFEM and the bubble-stabilized LSFEM with the exact solution for Hartmann numbers $M = 100$ and $M = 500$, respectively, at several grid points in the first quadrant of the channel. One can find that the primitive LSFEM is not able to achieve acceptable results even for such relatively small Hartmann numbers. Indeed, its performance is getting worse when M is getting larger. However, the bubble-stabilized LSFEM exhibits accurate and stable results that are comparable with the exact solution. The superior performance of the bubble-stabilized LSFEM will be demonstrated in the next two examples, where we consider much larger Harmann numbers, e.g. $M = 1/\kappa = 10^4, 10^6$.

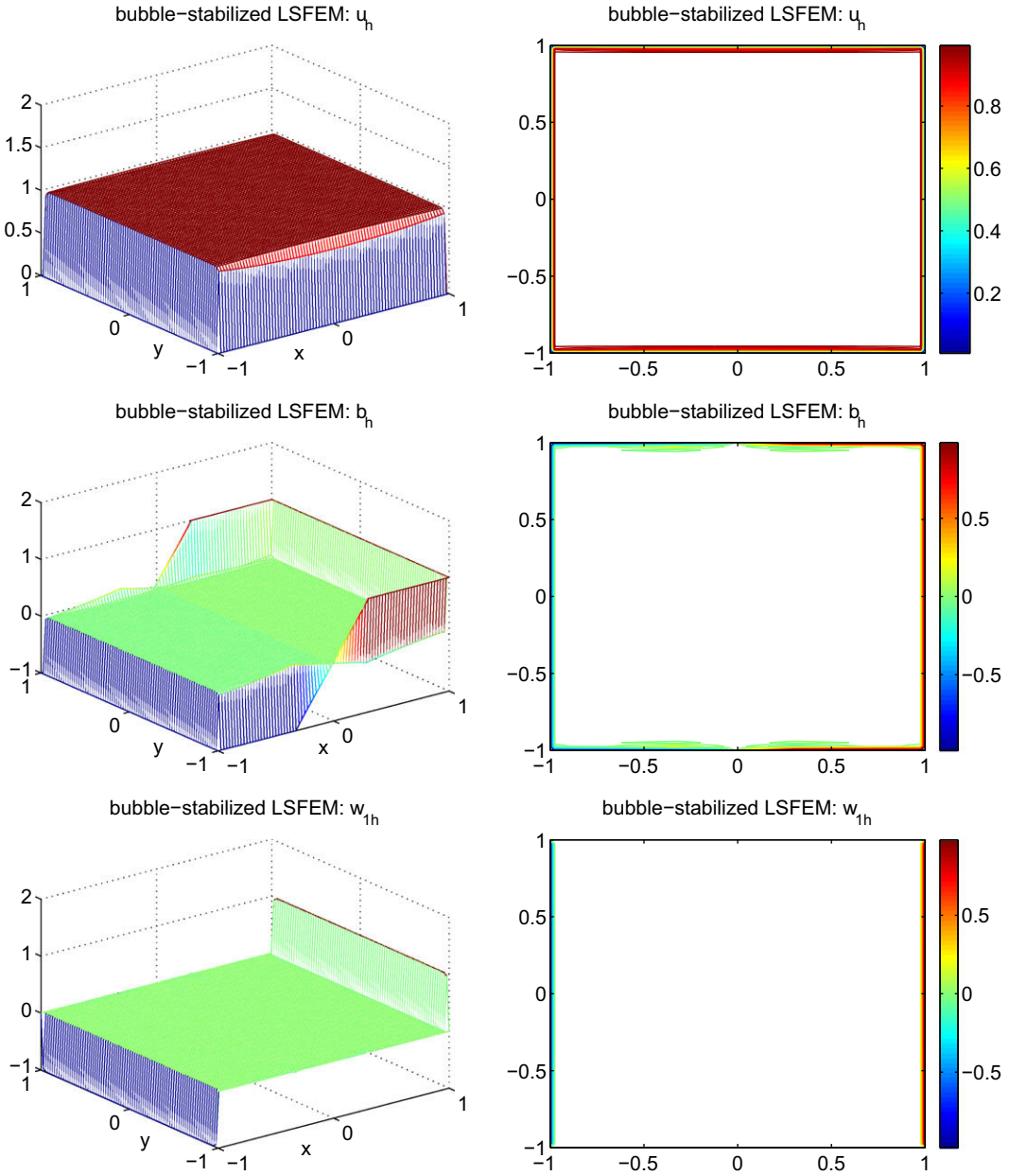

Fig. 5.7. Numerical solutions obtained by the bubble-stabilized LSFEM for Example 5.3 with $\kappa = 10^{-4}$.

Example 5.2 (*The 2D square-channel flow with an oblique applied magnetic field*). We consider the same problem with Example 5.1, except the externally applied magnetic field makes various positive angles α with the x-axis (see Fig. 5.2) and $\kappa = 10^{-4}$. Numerical computations are carried out for values of $\alpha = \pi/4, \pi/3$ and $\pi/2$, respectively. The elevation and contour plots for approximate solutions generated by the bubble-stabilized LSFEM are depicted in Figs. 5.3, 5.4 and 5.5. One can observe that when the external magnetic field applies obliquely, the boundary layers are concentrated near the corners in the direction of the field for both solutions u and b. This is a well-known behavior of the MHD flow [21].

Example 5.3 (*The 2D square-channel flow driven by the current produced by electrodes*). We examine the MHD flow in the 2D square-channel driven by the current produced by electrodes, placed one in each of the walls of the duct where the applied magnetic field b_0 is perpendicular (see Fig. 5.6). In this example, $f = g = 0$. The boundary conditions are given by

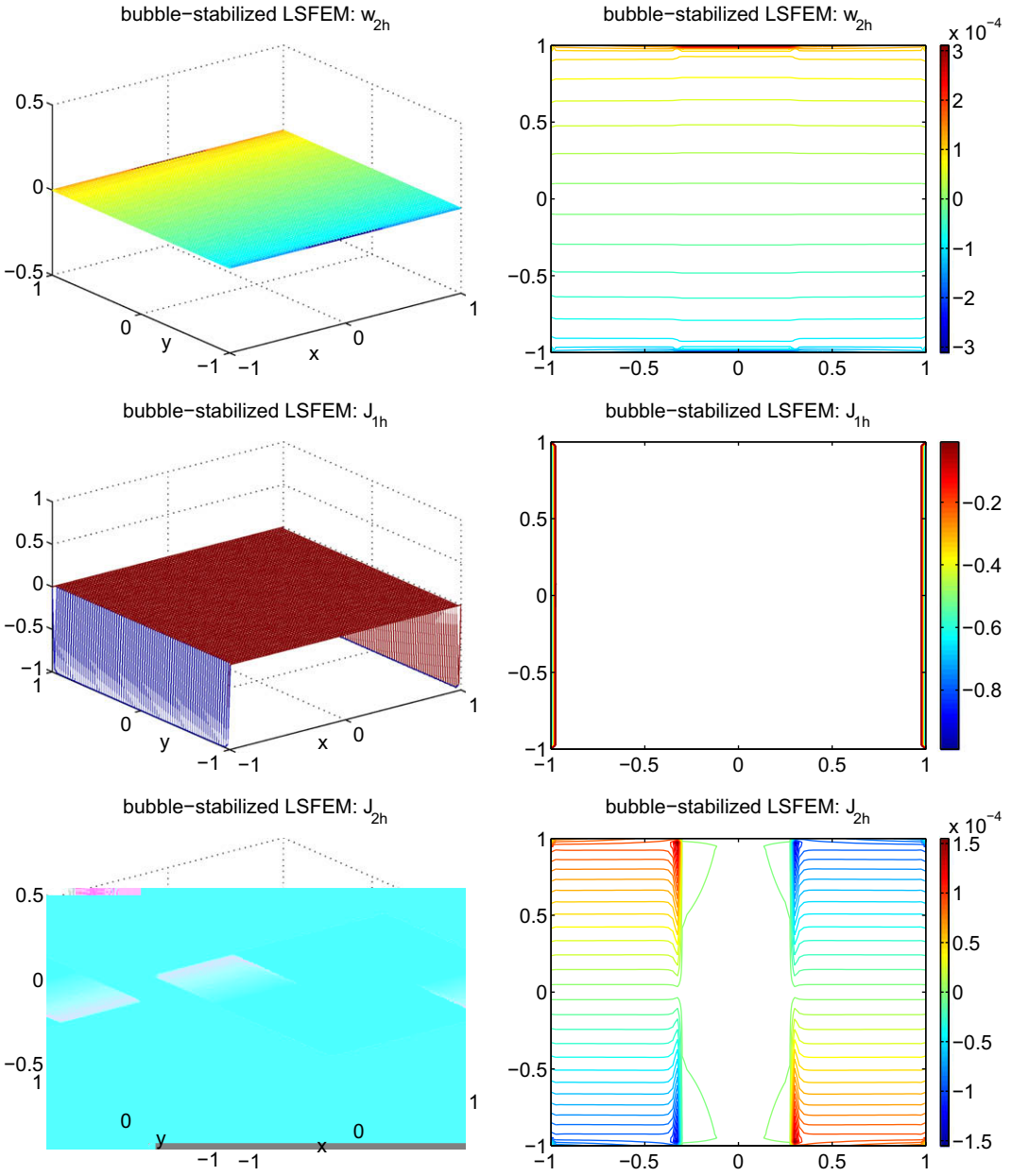

Fig 5.7. *(continued)*

$$\begin{cases} u = 0 & \text{on } \partial\Omega, \\ b = p & \text{on } \{(x,y) \in \partial\Omega : x > \ell, y = \pm 1\} \cup \{(x,y) : x = 1, -1 \leqslant y \leqslant 1\}, \\ b = -p & \text{on } \{(x,y) \in \partial\Omega : x < -\ell, y = \pm 1\} \cup \{(x,y) : x = -1, -1 \leqslant y \leqslant 1\}, \\ \mathbf{J} \cdot \boldsymbol{n} = 0 & \text{on } \{(x,y) \in \partial\Omega : -\ell \leqslant x \leqslant \ell, y = \pm 1\}. \end{cases}$$

In numerical computations, we set $\ell = 0.3, p = 1$ and then consider $\kappa = 10^{-4}$ and $\kappa = 10^{-6}$, respectively. The elevation and contour plots for approximate solutions generated by the bubble-stabilized LSFEM are displayed in Figs. 5.7 and 5.8. It can be observed, from these figures, that boundary layer formation makes a strong appearance for u, b, ω_1 and J_1. Though the approximate solutions u_h and b_h exhibit a little bit oscillatory behavior near the boundaries $y = \pm 1$, the bubble-stabilized LSFEM still presents an attractive performance for high Hartmann number at least up to $M = 10^6$ (i.e., $\kappa = 10^{-6}$).

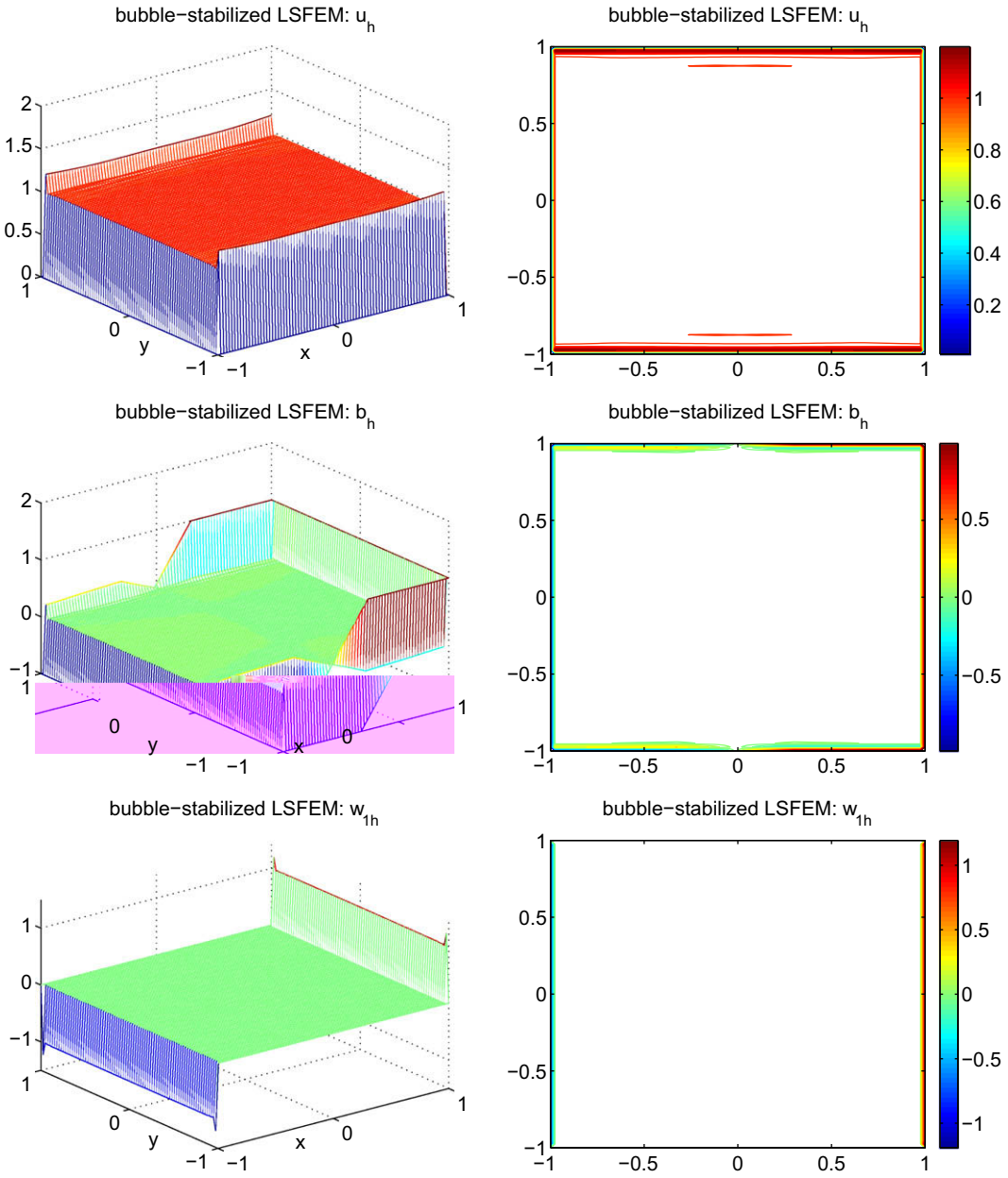

Fig. 5.8. Numerical solutions obtained by the bubble-stabilized LSFEM for Example 5.3 with $\kappa = 10^{-6}$.

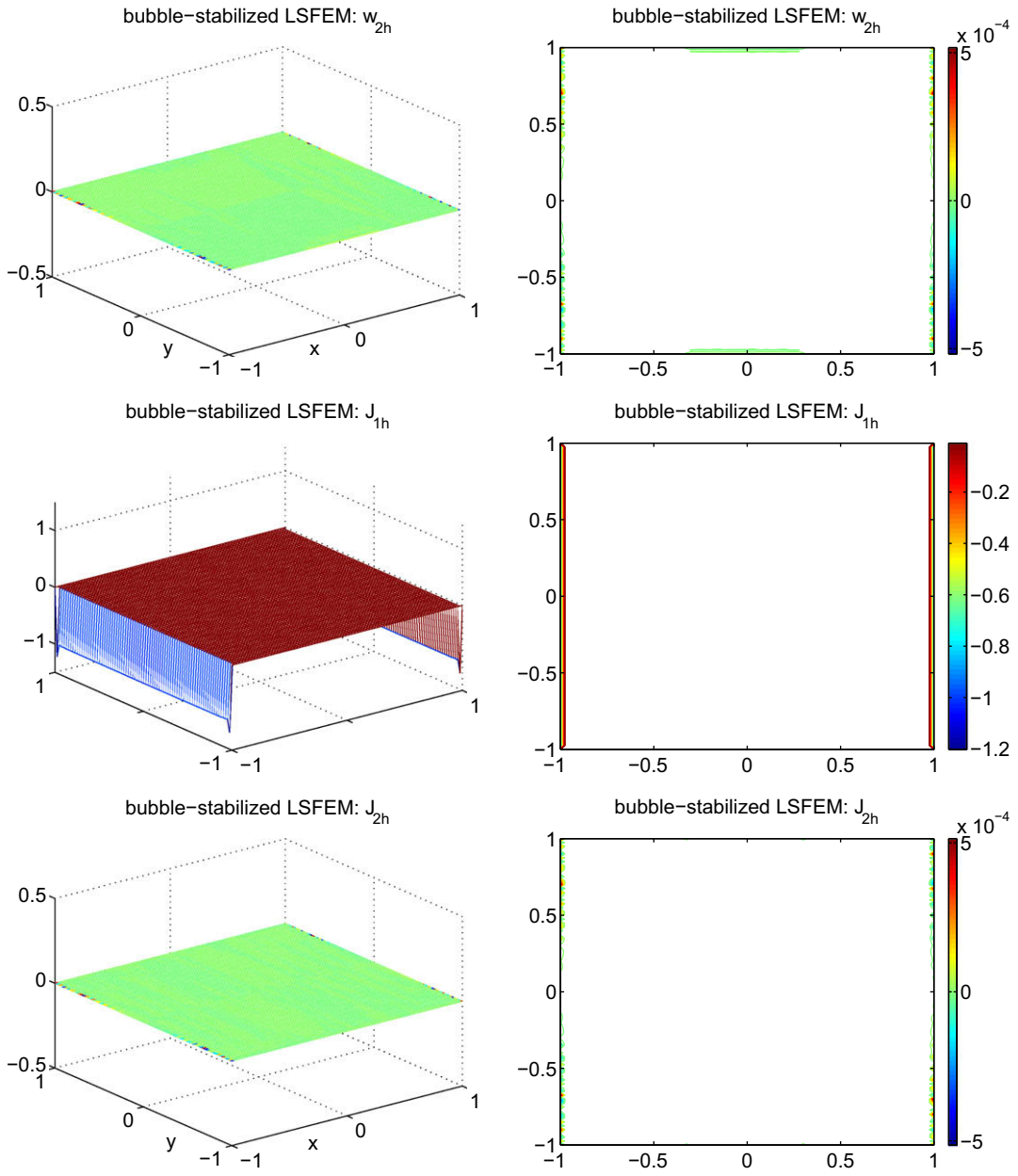

Fig 5.8. *(continued)*

6. Summary and conclusions

In this paper, we have proposed a novel stabilized least-squares finite element method using the residual-free bubble functions for approximating the solution of the MHD duct flow at high Hartmann number, which is a convection-dominated convection–diffusion problem. The most distinguished features of this approach are that the resulting linear system is symmetric and positive definite, and this bubble-stabilized LSFEM is capable of resolving high gradients near the layer regions without refining the mesh. We have shown that this approach gives more accurate and stable results even for high values of the Hartmann number. Numerical results are presented for several examples including the Shercliff problem which possesses an analytic solution.

In order to gain the residual-free bubble functions, the Galerkin least-squares method is applied to solve the corresponding local problems on elements. Therefore, we indeed have introduced a two-level finite element method consisting of a mesh for discretization and a submesh for approximating the computations of the residual-free bubbles. Apparently, the

approximations of the bubble functions can be obtained simultaneously by using parallel computations to accelerate the solution process.

Recently, the multiscale finite element approach [17] has been applied to the single-equation convection-dominated problems (cf. [8,14]). This approach is designed to efficiently capture the large scale behavior of the solution without resolving all the small scale features. This is accomplished by constructing the multiscale finite element basis functions that are adaptive to the local property of the differential operator [17]. This methodology is very close to the finite element method enriched with the bubble functions and clearly, the underlying idea can be employed for solving the MHD duct flow problems. A further study in this direction is in progress and we will report the results elsewhere.

Acknowledgment

The authors would like to thank the editor, Professor Tang, and the anonymous referees for their valuable comments and suggestions. This work was partially supported by the National Science Council of Taiwan.

References

[1] P.B. Bochev, M.D. Gunzburger, Analysis of least-squares finite element methods for the Stokes equations, Math. Comput. 63 (1994) 479–506.
[2] P.B. Bochev, M.D. Gunzburger, Finite element methods of least-squares type, SIAM Rev. 40 (1998) 789–837.
[3] S.C. Brenner, L.R. Scott, The Mathematical Theory of Finite Element Methods, Springer-Verlag, New York, 1994.
[4] F. Brezzi, A. Russo, Choosing bubbles for advection–diffusion problems, Math. Models Meth. Appl. Sci. 4 (1994) 571–587.
[5] F. Brezzi, L.P. Franca, A. Russo, Further considerations on residual-free bubbles for advective–diffusive equations, Comput. Methods Appl. Mech. Engrg. 166 (1998) 25–33.
[6] F. Brezzi, T.J.R. Hughes, L.D. Marini, A. Russo, E. Süli, A priori error analysis of residual-free bubbles for advection–diffusion problems, SIAM J. Numer. Anal. 36 (1999) 1933–1948.
[7] Z. Cai, R. Lazarov, T.A. Manteuffel, S.F. McCormick, First-order system least-squares for second-order partial differential equations: Part I, SIAM J. Numer. Anal. 31 (1994) 1785–1799.
[8] A. Cangiani, E. Süli, Enhanced RFB method, Numer. Math. 101 (2005) 273–308.
[9] C.L. Chang, B.-N. Jiang, An error analysis of least-squares finite element method of velocity-pressure-vorticity formulation for Stokes problem, Comput. Methods Appl. Mech. Engrg. 84 (1990) 247–255.
[10] C.L. Chang, Finite element approximation for grad-div type systems in the plane, SIAM J. Numer. Anal. 29 (1992) 452–461.
[11] J.M. Deang, M.D. Gunzburger, Issues related to least-squares finite element methods for the Stokes equations, SIAM J. Sci. Comput. 20 (1998) 878–906.
[12] L.P. Franca, S.L. Frey, T.J.R. Hughes, Stabilized finite element methods: I. application to the advective–diffusive model, Comput. Methods Appl. Mech. Engrg. 95 (1992) 253–276.
[13] L.P. Franca, A. Nesliturk, M. Stynes, On the stability of residual-free bubbles for convection–diffusion problems and their approximation by a two-level finite element method, Comput. Methods Appl. Mech. Engrg. 166 (1998) 35–49.
[14] L.P. Franca, J.V.A. Ramalho, F. Valentin, Multiscale and residual-free bubble functions for reaction-advection–diffusion problems, Int. J. Multiscale Comput. Engrg. 3 (2005) 297–312.
[15] L.P. Franca, G. Hauke, A. Masud, Revisiting stabilized finite element methods for the advective–diffusive equation, Comput. Methods Appl. Mech. Engrg. 195 (2006) 1560–1572.
[16] V. Girault, P.A. Raviart, Finite Element Methods for Navier–Stokes Equations: Theory and Algorithms, Springer-Verlag, New York, 1986.
[17] T.Y. Hou, X.-H. Wu, A multiscale finite element method for elliptic problems in composite materials and porous media, J. Comput. Phys. 134 (1997) 169–189.
[18] T.J.R. Hughes, L.P. Franca, G.M. Hulbert, A new finite element formulation for computational fluid dynamics: VIII the Galerkin/least-squares method for advective–diffusive equations, Comput. Methods Appl. Mech. Engrg. 73 (1989) 173–189.
[19] B.-N. Jiang, The Least-Squares Finite Element Method, Springer-Verlag, Berlin, 1998.
[20] S.-C. Kao, Some Residual-Free Bubble Enrichment Least-Squares Finite Element Method for the Convection–Diffusion Equation, Master Thesis, National Central University, Taiwan, July 2008.
[21] A.I. Nesliturk, M. Tezer-Sezgin, The finite element method for MHD flow at high Hartmann numbers, Comput. Methods Appl. Mech. Engrg. 194 (2005) 1201–1224.
[22] A.I. Nesliturk, M. Tezer-Sezgin, Finite element method solution of electrically driven magnetohydrodynamic flow, J. Comput. Appl. Math. 192 (2006) 339–352.
[23] A.I. Pehlivanov, G.F. Carey, R.D. Lazarov, Least-squares mixed finite elements for second-order elliptic problems, SIAM J. Numer. Anal. 31 (1994) 1368–1377.
[24] R. Scandiuzzi, B.A. Schrefler, FEM in steady MHD duct flow problems, Int. J. Numer. Meth. Engng. 30 (1990) 647–659.
[25] B. Singh, J. Lal, FEM in MHD channel flow problems, Int. J. Numer. Meth. Engng. 18 (1982) 1104–1111.
[26] B. Singh, J. Lal, FEM for unsteady MHD flow through pipes with arbitrary wall conductivity, Int. J. Numer. Meth. Fluids 4 (1984) 291–302.